

Using coherence to measure two-time correlation functions

Mark Sutton and Khalid Laaziri

Regroupement québécois sur les matériaux de pointe and Department of Physics, McGill University, Montreal, Quebec, Canada H3A 2T8

mark@physics.mcgill.ca, laazirik@physics.mcgill.ca

F. Livet and F. Bley

LTPCM-ENSEEG-INPG, UMR-CNRS n° 5614, B.P. 75 - 38402 Saint Martin d'Hères CEDEX - FRANCE

flivet@ltpcm.inpg.fr, fbley@ltpcm.inpg.fr

Abstract: An introduction to x-ray intensity fluctuation spectroscopy is given by describing its relationship to speckle from coherent sources. Its use to measure two-time correlation functions is demonstrated using the equilibrium fluctuations of gold colloids in polystyrene and for non-equilibrium fluctuations in the unmixing below the miscibility gap in AILi.

© 2003 Optical Society of America

OCIS codes: (030.6140) Speckle; (290.5820) Scattering measurements; (340.7480) X-rays

References and links

1. Wyn Brown, editor, *Dynamic Light Scattering: The method and some applications* (Clarendon Press, Oxford 1993).
2. B. J. Berne and R. Pecora, *Dynamic Light Scattering* (Academic Press, Orlando, FL, 1976).
3. M. Sutton, S. E. Nagler, S. G. J. Mochrie, T. Greytak, L. E. Bermann, G. Held, G. B. Stephenson, "The Observation of Speckle by Diffraction with Coherent X-rays," *Nature* **352**, 608-610 (1991).
4. S. Brauer, G. B. Stephenson, M. Sutton, R. Brüning, E. Dufresne, S. G. J. Mochrie, G. Grübel, J. Als-Nielsen, D. L. Abernathy, "X-ray intensity fluctuation spectroscopy observations of critical dynamics in Fe₃Al," *Phys. Rev. Lett.* **74**, 2010-2013 (1995).
5. S. Dierker, R. Pindak, R. M. Fleming, I. K. Robinson and L. E. Berman, "X-Ray Photon Correlation Spectroscopy Study of Brownian Motion of Gold Colloids in Glycerol," *Phys. Rev. Lett.* **75**, 449-552 (1995).
6. T. Thurn-Albrecht, W. Steffen, A. Patkowski, G. Meier, E. W. Fischer, G. Grübel and D. L. Abernathy, "Photon Correlation Spectroscopy of Colloidal Palladium Using a Coherent X-Ray Beam," *Phys. Rev. Lett.* **77**, 5437-5440 (1996).
7. M. Sutton, "Coherent X-ray Diffraction," in *Third-Generation Hard X-ray Synchrotron Radiation Sources: Source Properties, Optics, and Experimental Techniques*, Dennis M. Mills ed. (John Wiley and Sons, Inc, New York, 2002), Chap. 3.
8. D. J. Pine, D. A. Weitz, P. M. Chaikin, and E. Herbolzheimer, "Diffusing Wave Spectroscopy," *Phys. Rev. Lett.* **60**, 1134-1137 (1988).
9. A. R. Sandy, L. B. Lurio, S. G. J. Mochrie, A. Malik, G. B. Stephenson, J. F. Pelletier and M. Sutton, "Design and Characterization of an Undulator Beamline Optimized for Small-Angle Coherent X-ray Scattering at the Advanced Photon Source," *J. Synch. Rad.* **6**, 1174-1184 (1999).
10. D. Lumma, L. B. Lurio, S. G. J. Mochrie and M. Sutton, "Area detector based photon correlation in the regime of short data batches: data reduction for dynamic x-ray scattering," *Rev. Sci. Inst.* **71**, 3274-3289 (2000).
11. M. K. Corbierre, N. S. Cameron, M. Sutton, S. G. J. Mochrie, L. B. Lurio, A. Rhüm and R. B. Lennox, "Polymer-Stabilized Gold Nanoparticles and Their Incorporation into Polymer Matrices," *J. Am. Chem. Soc.* **123**, 10411-10412 (2001).
12. M. K. Corbierre, N. S. Cameron, M. Sutton, K. Laaziri, "Polymer-Stabilized Gold Nanoparticles and Their Incorporation into Polymer Matrices," in preparation.
13. K. Schätzle, "Single photon correlation techniques," in *Dynamic Light Scattering: The method and some applications*, Wyn Brown, ed. (Clarendon Press, Oxford 1993), Chap. 2.

14. E. Geissler, "Dynamic light scattering from polymer gels," in *Dynamic Light Scattering: The method and some applications*, Wyn Brown, ed. (Clarendon Press, Oxford 1993), Chap. 11.
 15. B. Crosignani, P. Di Porto and M. Bertolotti, *Statistical Properties of Scattered Light* (Academic Press, New York 1975), Sect. V.5.
 16. A. Malik, A. R. Sandy, L. B. Lurio, G. B. Stephenson, S. G. J. Mochrie, I. McNulty and M. Sutton, "Coherent X-ray Study of Fluctuations During Domain Coarsening," *Phys. Rev. Lett.* **81**, 5832-5835 (1998).
 17. F. Livet, F. Bley, R. Caudron, D. Abernathy, C. Detlefs, G. Grübel and M. Sutton, "Kinetic evolution of unmixing in an AlLi alloy using x-ray intensity fluctuations spectroscopy," *Phys. Rev. E* **63**, Article 036108 (7 Pages) (2000).
 18. G. Brown, P. A. Rikvold, M. Sutton and M. Grant, "Speckle from phase-ordering systems," *Phys. Rev. E* **56**, 6601-6612 (1997).
 19. G. Brown, P. A. Rikvold, M. Sutton and M. Grant, "Evolution of speckle during spinodal decomposition," *Phys. Rev. E* **60**, 5151-5162 (1999).
 20. L. Cipelletti and D. A. Weitz, "Ultralow-angle dynamic light scattering with a charge coupled device camera based multispeckle, multitau correlator," *Rev. Sci. Instr.* **70**, 3214-3221 (1999).
 21. E. Geissler, A-M. Hecht, C. Rochas, F. Bley, F. Livet and M. Sutton, "Aging in a filled polymer: Coherent small angle x-ray and light scattering," *Phys. Rev. E* **62**, 8308-8313 (2000).
-

1. Introduction

After a brief discussion of microstructure, this article gives an intuitive introduction to dynamic light scattering (DLS) also called intensity fluctuation spectroscopy (IFS). IFS measures the temporal correlations in diffraction intensities and these can usually be simply related to temporal correlations of density fluctuations. In equilibrium systems, these correlation functions depend only on the time difference between measurements and are independent of any origin for time. Thus, IFS reduces to measuring one-time correlation functions. In non-equilibrium systems, these intensity correlations depend on both time arguments and full two-time correlation functions are measured. In this context, an example of IFS using x-rays will be given for an equilibrium system. This example is presented to show how array detectors and the isotropy of scattering allows one to measure two-time correlation functions. A second example in which IFS is used to measure two-time correlation functions in a non-equilibrium system is then given. This article emphasizes what is involved in measuring these two-time correlation functions and the science underlying their behaviour is left to the references.

The physical properties of a material are most often controlled by its microstructure rather than its atomic structure. Control of this microstructure by specialized heat treatments and other techniques is the reason for many of the steps in modern materials processing. The simple observation that a material's properties depends on its history shows that these are non-equilibrium phenomena. Because of this importance, measurements of microstructure play a unique role in understanding the interplay between a material's structure and its properties. Scattering, primarily using x-rays and neutrons, plays a leading role in measuring structure covering the length scales from atomic distances to distances involved in a material's microstructure. Scattering with both visible photons and electrons have also made many significant contributions in this area, but we have singled out x-rays and neutrons because their interactions with matter allow more detailed structural measurements (exemplified by their predominant use in crystallography). Inelastic measurements, probing the energy levels of a system, have given deep insight into the dynamics of the atoms in a material, but have not been as useful in studies of microstructure. This is, in part, due to the small fraction of the atoms that are directly affected by the microstructure and also by the long time scales (and thus low energies) that are associated with its evolution. Measuring dynamics in time, rather than in energy, overcomes (or sidesteps) these energy resolution issues for probes which are sensitive to the appropriate length scales. Typically, these length scales are in the few nanometers to several micron range. (Following current trends, one should probably call it nanostructure not microstructure.) Dynamic light

scattering [1, 2] provides a powerful probe that measures time fluctuations (at least in transparent systems) but it can be limited by the wavelength of visible light and often doesn't quite reach the shorter length scales needed. The recent extension to x-rays (XIFS) is proving to be a powerful way to explore this type of behaviour[3, 4, 5, 6, 7].

XIFS is an x-ray diffraction technique. As such, the intuition and expertise that has been developed for diffraction carries over to this new technique. The extra information in XIFS comes from exploiting coherence properties of the incident radiation which leads to an effect called *speckle*. Speckle, often seen in laser light, results when coherent light reflects or scatters diffusely off disordered material. The intensity at each spot in the "image" is the result of light scattered (reflected) from many different points of the disordered materials. The essentially random path lengths of the light from these points in the sample to the point in the image, leads to the light being the sum of rays with a random set of phases. However, even though it is randomly distributed from point to point, the phase at any point sums to a definite value since the incident light is coherent. Where phases add destructively there are dark spots and where they add constructively bright ones. Hence, the speckled appearance of the image. From this description, one should be able to convince oneself, that for diffraction, the speckle pattern is simply the appropriate projection of the Fourier transform of the scattering volume. The requirement of a disordered material, that is one composed of small random parts, gives rise to a much broader diffraction pattern which is modulated by this speckle. A conventional diffraction pattern, as taken with an incoherent beam, has the finer speckle pattern smeared out by the angular spread of the incident beam (transverse incoherence) or by the wavelength spread (longitudinal incoherence) or by a combination of both.

IFS can now be explained by imagining that the diffracting material fluctuates in time and thus so do the speckle intensities. Hence the name IFS. Note that the fluctuating intensities even occur in equilibrium systems where the conventional diffraction pattern is constant in time. IFS is an ideal way to study the kinetics of fluctuations in a system provided that the scattering intensity is sufficient for the time scales of the system under study. For the last three decades or so, it has been extensively used with light scattering to study a large variety of systems [1]. For x-rays, IFS has the advantages of accessing optically opaque materials, of probing shorter length scales and of being less affected by multiple scattering (see, however, a description of diffusing wave spectroscopy [8]). The prime disadvantage of x-rays over visible light is the much lower coherent intensity levels of x-ray sources.

We conclude this section with a summary of the criteria for XIFS, for more details see Refs. [9, 10, 7]. (1) The coherence conditions determine a coherence volume and the observed scattering must come from this volume. In the paraxial limit, the volume is usually determined by the finite size of the source and by its monochromaticity. There are two transverse coherence lengths which depend on the horizontal and vertical root mean square (rms) size of the source σ_h , σ_v . At a distance R from the source, $\xi_i = \lambda R / (2\pi\sigma_i)$ are the rms transverse coherence sizes (we have used $\sigma_i \ll R$). The longitudinal coherence length $\xi_l = \lambda^2 / (2\Delta\lambda) = c / (2\Delta\nu)$ specified by either wavelength λ with spread $\Delta\lambda$ or frequency ν with spread $\Delta\nu$. More precisely, the longitudinal coherence limits the largest path length difference between points in the scattering volume. For reflection geometry this constraint is approximately $\xi_l (k_i/q)^2$. Here $q = |\vec{q}| = |\vec{k}_o - \vec{k}_i|$ is the wave-vector probed and \vec{k}_i and \vec{k}_o are the incident and out-going wave-vectors. For transmission at small angles it is approximately $\xi_l k_i/q$. These sizes are typically several microns for undulator x-ray sources but the path length difference constraint may grow to millimetres for small angle scattering. (2) The detector resolution must resolve the speckle size. This is $\approx \lambda / \xi_i$, the diffraction broadening from the finite size of the beam. (3) Sufficient photons must be scattered per speckle during the characteristic time of the dynamics. Since IFS is a noise measurement, many independent time samples are needed for good statistics. A good

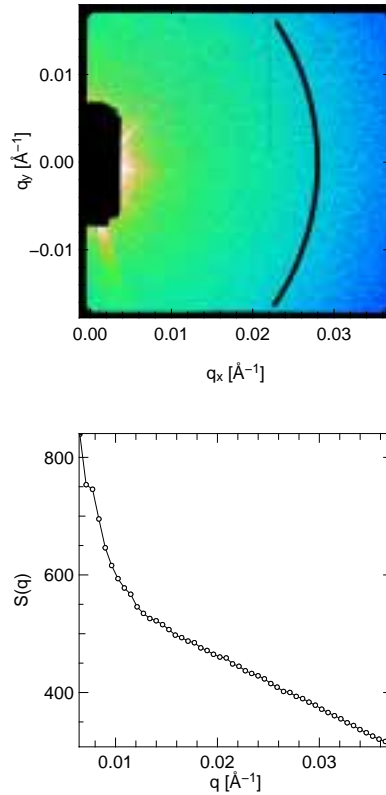


Fig. 1. (a) Scattering of Au particles in polystyrene (top). Black region is due to the shadow of a beam stop and the black arc consists of the wave-vectors for which fluctuations are shown ($q = .028\text{\AA}^{-1}$) in Fig. 2. The two directions of the wave-vector (horizontal and vertical) are labelled by q_x and q_y and $q = \sqrt{q_x^2 + q_y^2}$. (b) Circular average of (1a) (bottom). The 20 pixel wide stripe of the black arc contribute to the single point in this circular average for $q = .028(\pm .0003)\text{\AA}^{-1}$.

rule of thumb to estimate how short a time constant can be measured for a given scattering intensity is to require one count per speckle in each time constant. Since the scattering volume is small by (1), strong coherent x-ray sources such as third generation synchrotrons are needed. Typical results measure time constants from milliseconds to many minutes, for wave-vectors from 10^{-4} to 1 or 2 \AA^{-1} .

2. Equilibrium IFS

In this section we present data for the colloidal system of Au particles in the polymer polystyrene. We present this data to illustrate the above description more explicitly and in a way which leads to a natural description using IFS for non-equilibrium systems. The science of this interesting system will not be addressed [11, 12].

Particles in a homogeneous material lead to a peak in the small angle x-ray scattering (SAXS) which reflects the size and distribution of particle shapes. Figure 1(a) shows the small angle x-ray scattering from 60 nm gold particles well dispersed in polystyrene for 25 C, a temperature below the glass transition. The scattering pattern was collected on an area detector so a relatively large section of the small angle peak could be collected in parallel. The area detector

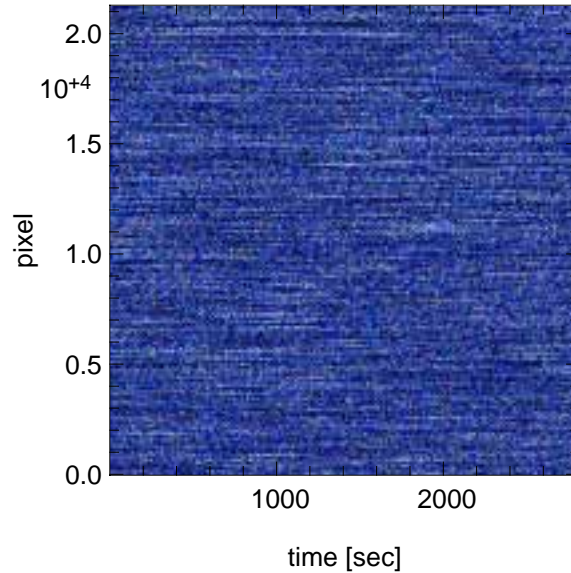


Fig. 2. The intensity fluctuations versus time for selected individual pixels from the 20 pixel wide arc of scattering at wave-vectors for which $|\vec{q}| = .028(+ - .0003)\text{\AA}^{-1}$. Increasing pixel number corresponds to increasing angle around the arc. Lighter colours are higher intensities.

is a charge coupled device (CCD) used with direct illumination. The wavelength used was 1.62\AA and each pixel in the CCD subtends an angle that corresponds to a wave-vector resolution of $3.1 \times 10^{-5} \text{\AA}^{-1}$. The black rectangular region center left is the shadow of a beam stop which prevents the transmitted incident beam from hitting the detector. Pixels near the edge of the CCD are also not used. The black arc will be discussed later. The top part of the figure shows the average scattering on the CCD and below is the corresponding circular average obtained by averaging the image over arcs of constant wave-vector. This circular average corresponds to what is usually measured in small angle scattering experiments. For this system the small angle scattering is isotropic and decays monotonically away from beam center. The size of the speckles for this setup is comparable to the pixel size of the CCD.

At this temperature, this system has a diffusion constant such that the time constants for the range of wave-vectors measured are of order minutes. The intensities in the CCD image fluctuate in time and this is illustrated in Fig. 2 which plots the intensities of several pixels in the black arc shown in Fig. 1(a) as a function of time. For an isotropic system, the time constants of the fluctuations depend only on the magnitude of the wave-vector and not on its direction. So each speckle should fluctuate with equivalent noise distributions and time constants. In this figure, the changing positions of the Au particles resulting from their Brownian motion leads to the observed intensity fluctuations. To analyze this noise one can measure its autocorrelation function,

$$g_2 = \langle I(t_1)I(t_2) \rangle / (\langle I(t_1) \rangle \langle I(t_2) \rangle), \quad (1)$$

where $\langle \dots \rangle$ denotes an average over pixels. If the intensities are uncorrelated, the g_2 will be equal to one and often $g_2 - 1$ is what is plotted. One can easily show that autocorrelating $(I(t_1) - \langle I(t_1) \rangle) / \langle I(t_1) \rangle$ will also result in $g_2 - 1$. Figure 3 shows two representations of these correlation functions. First, there is some freedom in how one chooses the pixels over which to average. Often different averages are used for $\langle I(t_1)I(t_2) \rangle$ and $\langle I(t) \rangle$. For $\langle I(t) \rangle$ one can choose more

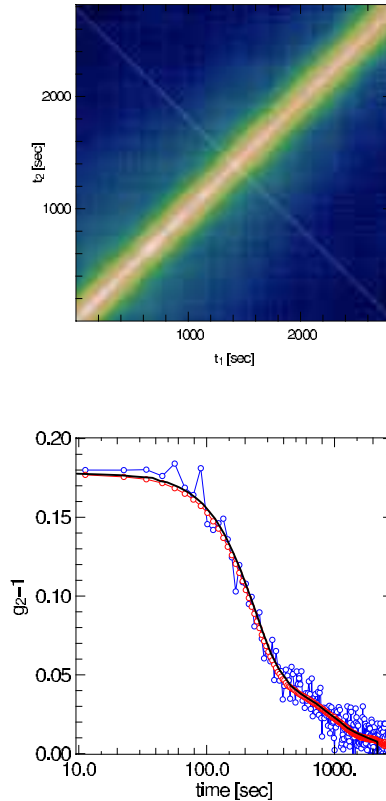


Fig. 3. (a) Two-time correlation functions, using averages over the arc in Fig. 1(a) (top). (b) Time correlation functions (bottom). The noisy signal (blue) is the single slice corresponding to the diagonal line in 3(a) (a function of $t_2 - t_1$). Since the function is symmetric in t_1 and t_2 only the portion for $t_2 > t_1$ is shown. The less noisy signal (red) is a simple average over all slices. The black curve on top is g_2 calculated using the multitau algorithm which obtains correlations for longer times after averaging intensities over successively longer times [13].

pixels to get a better estimate of the average scattering so for equilibrium scattering, averaging over time and over \vec{q} with the same $|\vec{q}|$ often leads to the best estimate. For Fig. 3(a) only averages over \vec{q} were performed showing that reasonable correlations can be measured from a pair of images. This is possible because of using array detectors. For equilibrium systems, the two-time correlation function only depends on $\tau = t_2 - t_1$. This is seen in Fig 3(a) by the colour contours being parallel to the diagonal. It is clear that better statistics can be obtained by appropriately averaging over time. Figure 3(b) shows correlation functions for one cut of Fig. 3(a) and superimposed on it are two ways of averaging over time.

Several comments about the correlation functions need to be mentioned. Thermal fluctuations are typically small variations about the average and so a Gaussian approximation for density fluctuations simplifies calculations [1, 2]. Also, quite generally in this limit, the time correlation functions are simple exponential decays, characterized by a single time constant.¹ Fourier transforming this into frequency space leads to the Lorentzian frequency spectrum often

¹Note, however, that this is typically not true for polymeric systems, and the correlation function in Fig. 3(b) is not a simple exponential [14].

observed by other techniques. Since we are measuring intensity-intensity correlation functions these are often the square of those for underlying thermodynamic fluctuations [1, 2].

We emphasise that intensity fluctuations are noise and as such a good estimate of the signal to noise is given by $1/\sqrt{N}$, where N is the number of uncorrelated times measured [13]. DLS measurements have typically measured the correlation functions at a single point of scattering and thus 10^4 correlation times are needed to get 1% accuracy. With the hundreds or even thousands of speckles measured in parallel by an appropriate area detector, correlation functions can be measured in only a few correlation times². This has an obvious advantage for measurements in systems with long correlation times such as seen in Fig. 3. Finally, two technical points. For $\langle I(t_1)^2 \rangle$ (i.e. $t_1 = t_2$), there is a contribution from photon statistics which does not appear in $\langle I(t_1)I(t_2) \rangle$ for $t_1 \neq t_2$. This can be removed by extrapolating the values on each side $t \pm \delta t$, δt being the time step. Also, the limit of $g_2(\tau) - 1$ as τ goes to zero would be 1.0 for a fully coherent beam and a lower value can result from various combinations of partial coherence in the experimental setup, a detector bigger than the speckle size or an indication that the system has time constants faster than the sampling time.

Using this analysis one can measure the correlation functions as a function of wave-vector. Access to larger wave-vectors is one of the advantages using x-rays for IFS. Measuring time constants as a function of wave-vector is closely related to the equation of motion of the system and is the motivation for making these types of measurements. We leave to the references a description of the wide variety of systems studied and the interesting science obtained but would like to point out that, for instance, the diffusion equation leads to time constants that vary as $1/D|\vec{q}|^2$.

3. Non-equilibrium IFS

Although extremely successful for equilibrium systems, IFS has not often been used to study fluctuations in non-equilibrium systems. This is in part due to the bias of DLS measurements to use point counting methods which require averaging over time to get good statistics and partly due to using autocorrelation techniques which depend on the average scattered intensity being constant. In non-equilibrium systems a full two-time correlation function needs to be measured and things are more difficult as these techniques can not be used. In a study of phase separation in a sodium borosilicate glass [16] and in the unmixing of AlLi [17], it was shown how to use an area detector and the isotropy of the x-ray scattering to overcome these limitations. Measuring many speckles at the same time not only helps with statistics but helps to decompose the time evolution of the scattering into an average and a fluctuating component³.

In the article we will present an example two-time correlation measurements from Livet *et al.* [17] to emphasize the above points. Please see the original articles for a comparison of the measurements [16, 17] to the predictions of dynamical scaling [18, 19]. These articles show the different nature of fluctuations in non-equilibrium systems.

Figure 4 shows the time evolution of the circular averaged SAXS pattern for the unmixing of $\text{Al}_{0.91}\text{Li}_{0.09}$ at 220 C. The sample was quickly quenched from 475 C above its miscibility gap to room temperature where everything is frozen. It was then heated *in-situ* to this anneal temperature which is below its miscibility gap but where diffusion constants are such that unmixing can take place on the time scale seen in the figure. The time at which the sample reached 220 C is defined as $t = 0$. For this isotropic system, an instantaneous average can be calculated by averaging over intensities at constant $|\vec{q}|$. Based on the high degree to which scaling works in the Al - Li system, this is equivalent to studying the fluctuations about an instantaneous "average"

²The required independence of each speckle is easily seen in the Gaussian approximation [15].

³Of course, if the fluctuating component is much faster than the variation in the average, a quasi-equilibrium approach may work.

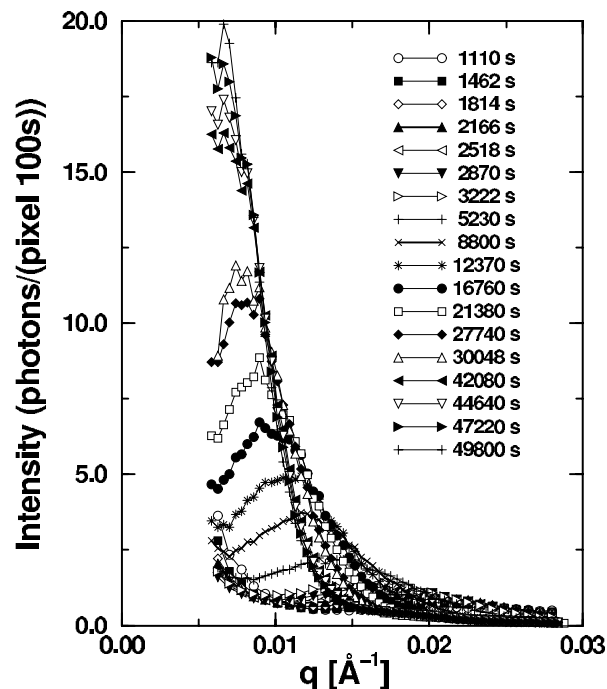


Fig. 4. Time evolution of scattered intensity. Scattering was measured with a wavelength of 1.51 Å.

as determined by the scaling form.

A two-time correlation function is presented in Fig. 5 for $|\vec{q}| = 0.0155 \text{ \AA}^{-1}$ and three of its cross-sections are shown in Fig 6. These correlation are based on autocorrelating:

$$D(\vec{q}, t) = \frac{I(\vec{q}, t) - \langle I(\vec{q}, t) \rangle}{\langle I(\vec{q}, t) \rangle}. \quad (2)$$

Here the averages are over 40 pixel wide annuli for the given time t , but calculations with 20 pixel annuli gave the same result aside from an increased Poisson noise. This figure clearly shows a dependence on both $t_2 - t_1$ and the average time from the quench $(t_1 + t_2)/2$, in clear contrast to Fig. 3(a). The growing width perpendicular to the diagonal shows the slowing down of the fluctuations with time.

Figure 6 shows three cross-sections for several values of constant t_1 . A fit to a theoretical form for the correlation function [18, 19] is also shown. This function is not a simple exponential and the figure shows both a Gaussian and Lorentzian form for comparison. The references discuss the comparison of these types of measurement to theories of dynamical scaling.

4. Conclusions

First, we conclude that by using area detectors, one can measure two-time correlation functions which are important in the study of non-equilibrium systems. The two examples of such measurements so far published [16, 17] have been in systems in which dynamical scaling was known to work well, but nothing in the measurement of the two-time functions depends on scaling. An obvious next step would be to extend these types of measurements to other examples of non-equilibrium systems. We also note that light scattering geometries exist [20, 21] which are also using CCD's and we would like to encourage their use for two-time correlations as well.

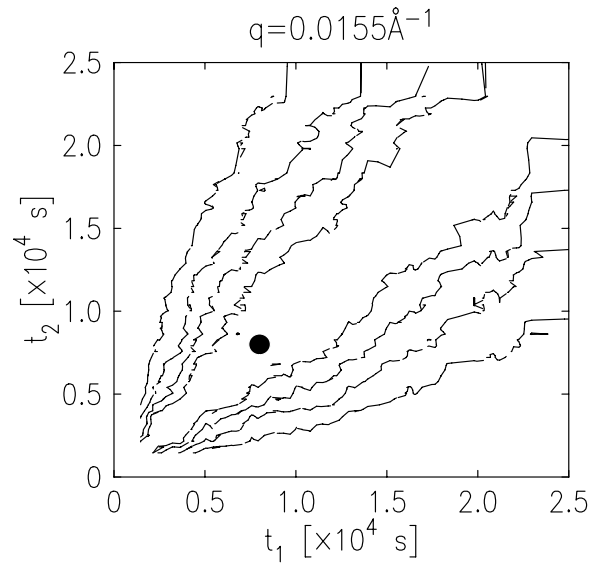


Fig. 5. Contour plots of two-time correlation functions for $|\vec{q}| = .1055$. Contour levels are 0.2, 0.4, 0.6 and 0.8. The diagonal $t_1 = t_2$ has been normalized to 1.0 after suppressing the effects of Poisson noise. The black dot indicates the time at which the peak maximum sweeps by this particular wave-vector.

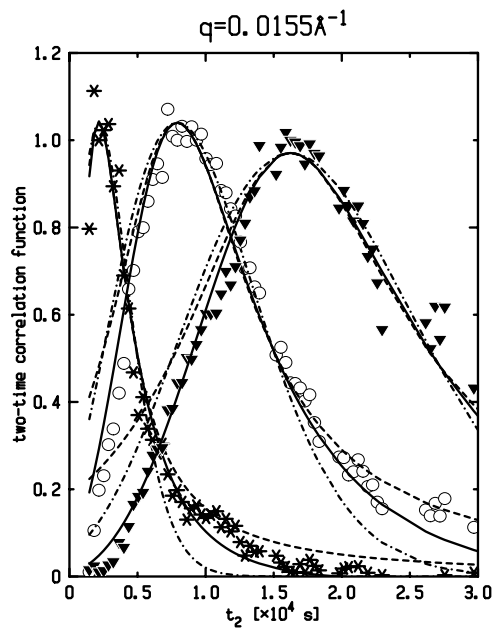


Fig. 6. Correlation functions for $q = .0155 \text{ \AA}^{-1}$ value and $t_1 = 2163 \text{ s}$; 7920 s ; 16230 s . Solid lines are the fits. For comparison, the dash-dot line is a Gaussian and dashed line is a Lorentzian with the same height and width as given by the fit.

Acknowledgements

The APS is supported by the DOE under contract No. W-31-109-Eng-38.

#2833 - \$15.00 US
(C) 2003 OSA

Received August 04, 2003; Revised September 15, 2003
22 September 2003 / Vol. 11, No. 19 / OPTICS EXPRESS 2277